Manufacture spectral responsivity of n-Fe_2O_3/p-Si heterojunction with effect Cl doping for high sensitive devices

H. K. Hassun[a], B. K. H. Al-Maiyaly[a], B. H. Hussein[a,*], Y. K. H. Moussa[b]
[a]*Department of physics, College of Education for Pure Science (Ibn Al-Haitham), University of Baghdad, Baghdad, Iraq*
[b]*Remote Sensing & GIS Department, College of Science, University of Baghdad, Baghdad, Iraq*

Visible-light photodetectors constructed Fe_2O_3 were manufactured effectively concluded chemical precipitation technique, films deposited on glass substrate and Si wafer below diverse dopant (0,2,4,6)% of Cl, enhancement in intensity with X-ray diffraction analysis was showed through favored orientation along the (110) plane, the optical measurement presented direct allowed with reduced band gap energies thru variation doping ratio , current–voltage characteristics Fe_2O_3 /p-Si heterojunction revealed respectable correcting performance in dark, amplified by way of intensity of incident light, moreover good photodetector properties with enhancement in responsivity occurred at wavelength between 400 nm and 470 nm.

(Received September 3, 2023; Accepted December 7, 2023)

Keywords: Iron(III) oxide, Photodetector, Optical band gap, Spectral responsivity

1. Introduction

Iron(III) oxide is the mineral composite through the formulation Fe_2O_3. Greatest of three mainly oxides of iron, existence iron(II) (FeO), besides iron(II,III) (Fe_3O4), which similarly arises certainly as the inorganic magnetite. By way of the inanimate identified by hematite, α -Fe_2O_3 is the foremost sources of iron in steel manufacturing [1]. Among various metal oxides, iron oxide was a lowest rate non-toxic situation responsive materials effortlessly available in nature [2], furthermore was a rhomb euhedrally center hexagonal construction by close pack lattice [3]. Similarly is an n-type semiconducting properties with optimum band gap of 2.1 eV for solar light absorption hence it was a talented materials for photo voltaic, photo catalytic then photo electrochemical application [4-6]. Fe_2O_3 displays wide ranges of requests for instance light induced water splitting [7] , catalysis[8], gas sensors [9], solar cells[10] and spin electronic devices[11]. In comparison with various methods for α-Fe2O3 nanostructures , chemical precipitation technique had numerous benefit for example low costs, shortest perpetrated time, squat react temperature, fine crystallize per highly purities products [12]. Up to now, insufficient study had been described on illumination detection through Fe_2O_3, photodetectors constructed in discrete Fe_2O_3 nan bridge among two Au electrode were testified, the devices presented faster response time of lower (20 ms) by a wavelength of 490 nm. The struggle to separated and facilities to recombined electron hole pair at Fe_2O_3 were mainly limitations. Additional improvement of the photo response presentations was required for useful applications [13]. Furthermore, Fe_2O_3 and Zn:Fe_2O_3 nanoparticles were organized thru sol-gel thru diverse Zn percentages. The photo degradation investigation displayed 87% of RB dye besmirched in 90 min associated toward 63% per pure Fe_2O_3 [14] , effective doping might meaningfully advance the movement of Fe_2O_3. Lately, Mg dopant Fe_2O_3 photocatalytic efficiency. Un dopant and doping Fe_2O_3 constructions were adult via two step electrochemically technique. Photocatalytic activities of 81% was gotten for the Mg: Fe_2O_3 nanostructures in 180 min, while Fe_2O_3 controlled lone 56% of deprivation [15].This work aims to manufacture (n- Cl: Fe_2O_3/p-Si) photo detector utilized chemical spry

* Corresponding author: boshra.h.h@ihcoedu.uobaghdad.edu.iq
https://doi.org/10.15251/JOR.2023.196.719

pyrolysis process then the characterizations for(n- Cl: Fe_2O_3/p-Si) and the fabrication photodetector were deliberated .

2. Experimental practice

Thin film (Fe_2O_3) were equipped by chemical spry pyrolysis deposition with thickness (400nm) , Iron nitrate aqueous material $Fe(NO_3)_3.9H_2O$ was used to prepare iron oxide thin films (Fe_2O_3) with a purity of 99%, ,the solution was prepared at a molar concentration (0.1M) by dissolving (4.0402gm) of the substance in (100ml) of purified water utilized a magnetic stirrer for a period of (15min) to ensure the homogeneity of the solution, and after completing the dissolution process, the solution was kept in a volumetric vial and left for (24hr) to ensure that there is no sediment or stuck in it. Also used (NH_4Cl) with a molecular weight of (53.49 gm / mol) with purity (99%) , when preparing the solution at a concentration of (0.1M) (0.5349 gm) was dissolved in (100 m l) of distill water utilized a magnetic mixer for period on (15 min), The Cl ratio was adjusted at (2,4,6)% , annealing procedure completed intimate furnace at (500 °C) for 1h. After preparing the thin films, their crystal structure and the effect of doping are identified by studying the X-ray diffraction pattern .The optical properties spectra were documented using of UV–VIS spectrophotometer "OPTIMA SP-3000" for wave length variety (200-1000) nm, besides with Tauc relative [16,17], the changed of direct band gap studied. Spectral responsivity regulate through utilized a mono chromatic light source through spectral variety (200‑900) nm.

3. Results and discussions

The influence of Cl dopant construction iron oxide compounds was scrutinized through X-ray diffraction. Figure ($1_{a,b,c,d}$) show four state explained different ratio (0,2,4,6)% for Cl, some diffraction peaks situated at 2θ = 33.14, 35.6, 54.11, and 62.3◦ experiential in the designs of the un doped besides Cl dopant Fe_2O_3 thin films, conforming to the (104), (110), (116), and (214) planes, individually, of characteristic Fe_2O_3 phase structured (rhombohedral, a = b = 5.023 Å, c = 13.70 Å where(JCPDS Card No. 01-089-8104) [18,19].

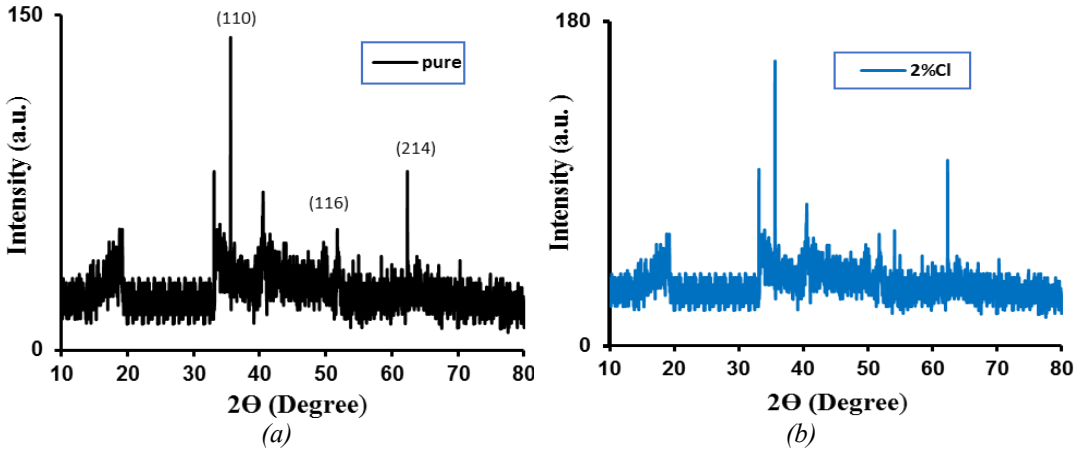

Fig. 1 a) b) XRD decorations of un doped plus Cl-dopant Fe_2O_3 thin films for different contents a) Pure, b)2% Cl

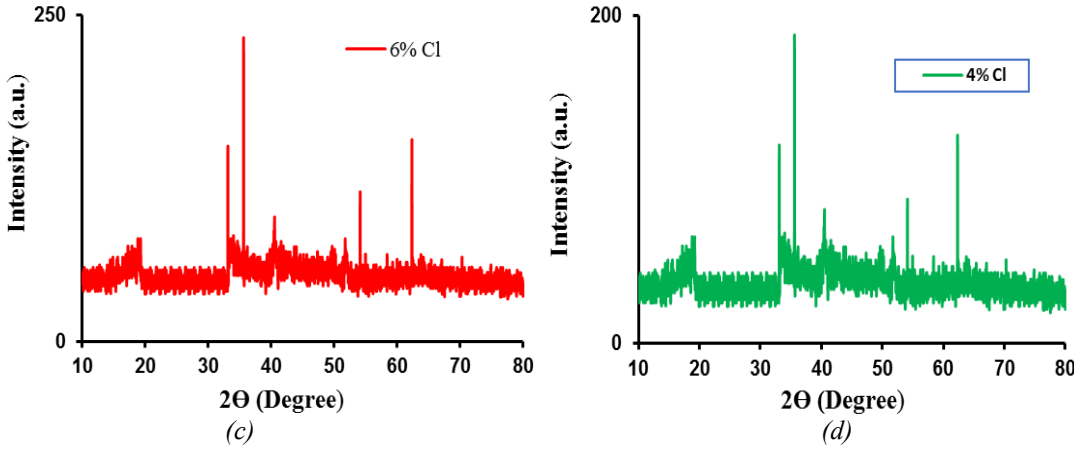

Fig. 1 c)d) XRD decorations of un doped plus Cl-dopant Fe_2O_3 thin films for different contents. c) 6% Cl, d) 4% Cl

Definitely not different peaks construction was detected, this approves high purity product and chlorine has effectively substituted into the Fe_2O_3 matrix. Investigation of X-ray demonstrations films are poly crystalline plus had a favored alignment sideways the (110) plane, similarly small shifts to highest diffraction angles were noticed of doped models, the variation with the doping concentration of Cl due to propensity of crystallized to change laterally the (110) plane growths thru the upsurge of the Cl dopant meditation active for 6 %.

The lattice factors a and c of the nanocrystals besides grain size D of completely the samples were assessed rendering to the equation (1) and Scherrer's formula [20,21]

$$\frac{1}{d^2} = \frac{4}{3}\left(\frac{h^2+hk+k^2}{a^2}\right) + \frac{l^2}{c^2} \quad (1)$$

where (hkl) are the Miller indices, the valued standards of lattice parameter are obtainable in Table 1. The considered standards of the unit cell parameter of cl dopent Fe_2O_3 were create to be subordinate than un doped films, which consequence in a decrease in the grain size .Chlorine combination produced local variations in the Fe_2O_3 environment, which approves the fruitful manufacture of Cl doping Fe_2O_3 thin film [22]. For additional Table (1) expression investigation of the influence of Cl dopant on the microstructure film.

Table 1. The disparity of grain size (D), unit cell volume (V) contrasted with Cl different ratio.

Cl %	a (Å)	c(Å)	V (Å)	hkl	D(nm)
o	5.034	13.77	302.1976	(110)	28.259
2	5.024	13.73	300.1238	(110)	27.822
4	5.024	13.72	299.9052	(110)	25.968
6	5.023	13.72	299.7858	(110)	25.355

Variation of the absorption coefficient by way of role of energy of the photon occurrence and the reflection as a function of the wave length of all films demonstration in figure (2) . It is clear from the results obtained that all films have higher values of the absorption coefficient, which designates a high probability of direct electronic transfers[23], we find that the modification in the absorption coefficient thru the photon energy of the Fe_2O_3 thin film is small by low energies, then the amount of change becomes greater and increases rapidly near the edge of optical absorption at the range of energies (2.55-4) eV, which reflects the presence of direct electronic transitions within this range of photon energies[24].

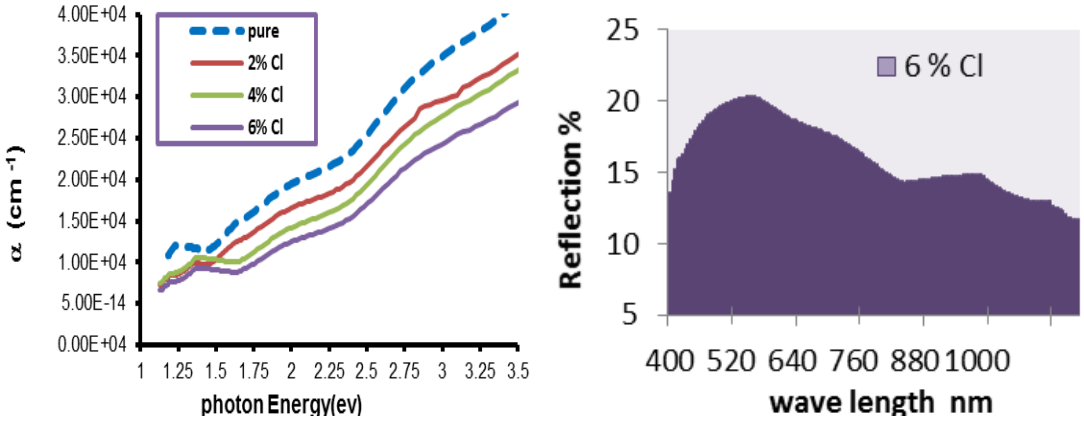

Fig. 2. The absorption coefficient (α) of undoped and Cl doped Fe_2O_3 and reflectance (R) for 6% Cl ratio.

It is noted from Figure, the values of the absorption coefficient decrease with increasing doping ratio, this is because the distortion process has generated scalable levels within the energy gap near the valence beam, reducing absorption.

The reflection information permits the estimate of the band gap standards done the discrepancy reflectance spectra for instance meaning of wavelength. According to Tauc

Formulas [25], the optical direct band gaps, values attained for iron oxide semiconductor and doping simple distinctive in figure (3), intensification of the direct transition rate through Cl dopant contented was experiential from (2.2 to 3.1) eV for pure and 6 % Cl doped Fe_2O_3 .We observed from figure decent connection with the crystallinities detected that identical doping percentage, where concentrated the structural defects. Also, absorption spectrum of all films displays an absorbance arrival nearby 500 nm and peak about 400 nm agreeing with 2.55 eV besides 3.1 eV, individually.

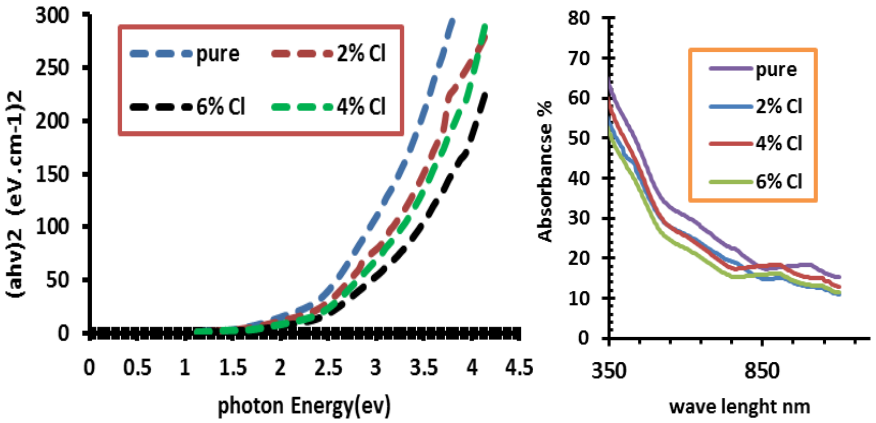

Cl %	0	2	4	6
Eg (eV)	2.55	2.78	2.92	3.1

Fig. 3. The optical band gaps and absorption spectrum of undoped and Cl doped Fe_2O_3 with different ratio.

(I-V) features of Fe_2O_3 / Si hetero junction photodetector in dark equally forward and reverse bias voltage show in figure (4). The forward current is proportional exponentially thru bias voltages which diffusion currents was the central constituent than recombination current.

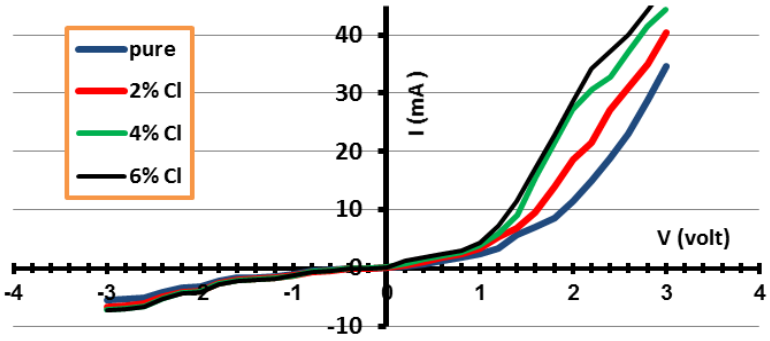

Fig. 4. Dark I–V features of n-Fe2O3 /p-Si heterojunction photodetector with (0,2,4,6)% Cl dopant ratio.

The illumination I-V characteristic of n-Fe2O3 /p-Si heterojunction photodetector at reverse bias was revealed in Figure (5). The cumulative of photocurrent through growing the reverse bias voltage dismiss qualified to the interior electric field laterally the depletion region where avoid the recombine photo produced electrons-holes. Below illumination per dissimilar power densities, (18,60, 100) mW/cm^2 , the photocurrent was create to be amplified thru light power as presented in Figure. This increasing in the photocurrent container stand correlated to photo produced carriers which cumulative the attentiveness of minor carriers controlling the photocurrent below reverse bias.

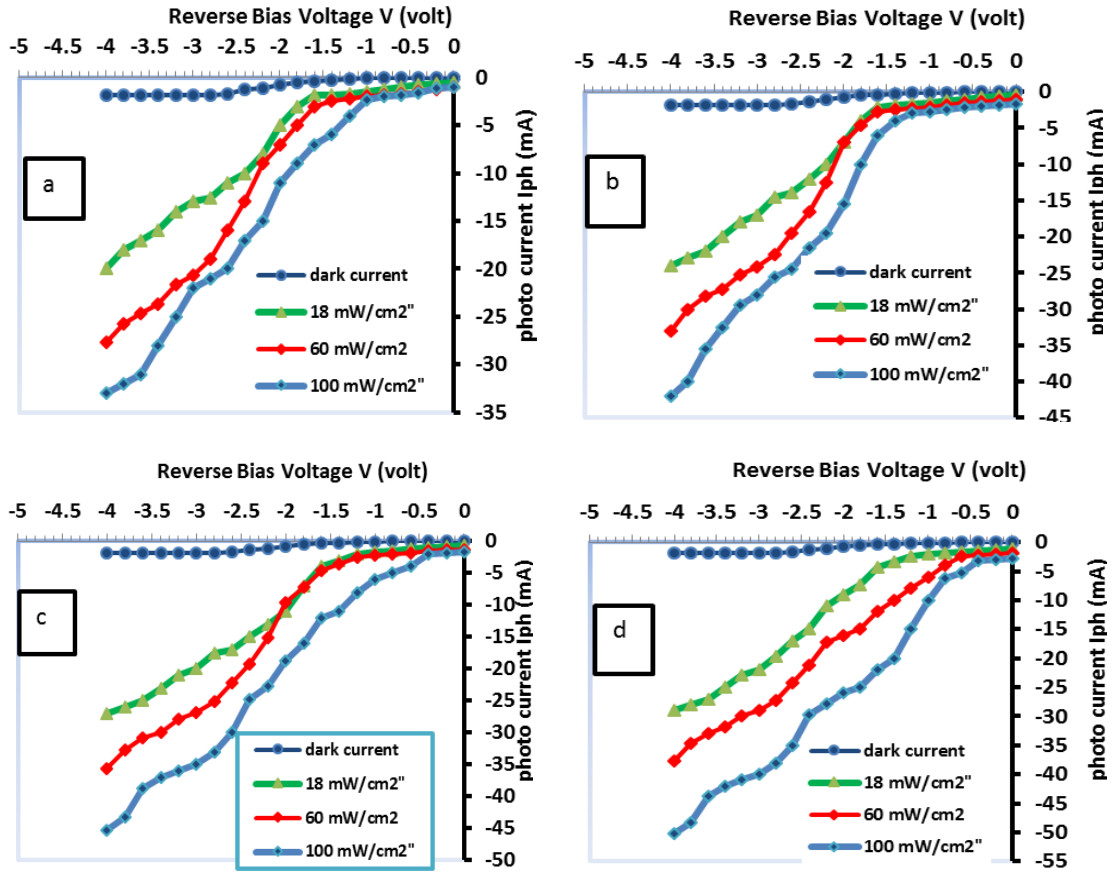

Fig. 5(a,b,c.d). Illumination (I-V) characteristic of n-Fe_2O_3 /p- Si hetrojunction photodetector with (0,2,4,6)% Cl dopant ratio respectively.

Figure (6) demonstrations the spectral response at (4V) reverse bias of pure Fe_2O_3 thin film based photodetector with (0,2,4,6)% Cl dopant ratio, the responsivity extending (400-1000) nm wavelength and defined by photocurrent generated per unit of power of the incident light intensity on active areas, version to equation [26]. The spectrum expressions wideband responses in the variety (400 - 700) nm, besides the responsivity of Fe_2O_3/Si photodetector was 0.571 A W^{-1} at 470 nm, the device displays a broadband sensitive cover the visible to near infrared district, the distinction of noise equivalent power as a function of wavelength for doped and undoped detectors was revealed in figure (7), the lowest NEP befalls as soon as spectral response has the maximum value, we can notice that NEP decreases when the films doping due to the defects which decrease with doping, and thus decrease noise current.

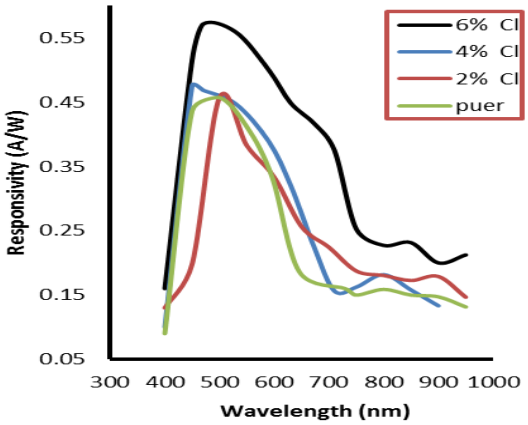

Fig. 6. The Spectral Responsivity of Fe_2O_3 /p-Si photodetector for dissimilar Cl doping percentage.

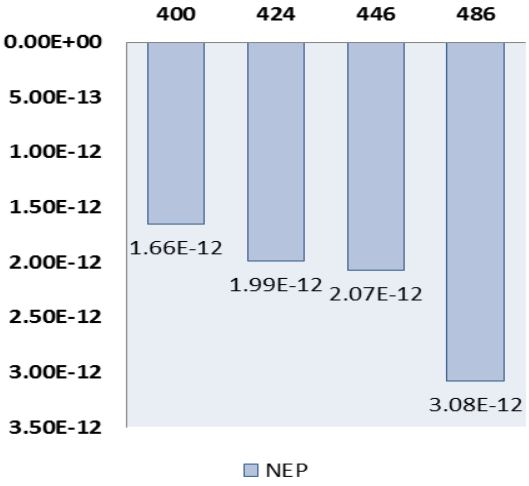

Fig. 7. The variation of noise equivalent power (NEP) thru wavelength Fe_2O_3 /p-Si photodetector at unrelated Cl doping ratio.

4. Conclusion

In summary, we attention on producing visible UV photodetectors and improvement the high response by enhancements on materials then structures. Fe_2O_3 and Cl doped Fe_2O_3were effectively manufactured by chemical spry pyrolysis method. A structural characterization revision shown that totally films are rhombohedral structure with (110) by means of primary orientation, where approves that Cl was fine combination for the Fe_2O_3 lattice, specifically for (6 % Cl). A direct band gap energy of rang (2.55-3.1) eV was assessed since absorption spectrum. The fabricated Fe_2O_3 /p-Si heterojunction revealed decent possessions thru spectral response, strong

absorption of Cl doped Fe_2O_3 in the visible light and peak response of (0.571 A/W) situated on (470 nm) for (6% Cl) .

References

[1] PubChem, Iron oxide (Fe2O3), hydrate, pubchem.ncbi.nlm.nih.gov. Retrieved 11 November 2020.

[2] P. Mallick, B.N. Dash, Nanosci. Nanotechnol. 3 (2013) 130-134.

[3] Cornell RM (2003) Schwertmann U, the Iron oxides, 2nd ed. WILEY-VCH GmbH & Co., KGaA, Weinheim

[4] Du H, Cao Y, Bai Y, Zhang P, Qian X, Wang D, Li T, Tang X (1998), J Phys Chem B 10:2329-2332; https://doi.org/10.1021/jp973056x

[5] Kouhbanani MAJ, Taghizadeh NBS, Amani AM, Alimardani V (2019), Adv Nat Sci Nanosci Nanotechnol 10:015007-015012; https://doi.org/10.1088/2043-6254/aafe74

[6] Dlugosch T, Chnani A, Muralidhar P, Schirmer A, Biskupek J, Strehle S (2017), Semicond Sci Technol 32:084001-084010; https://doi.org/10.1088/1361-6641/aa7593

[7] Catherine M. Aitchison, Reiner Sebastian Sprick, Andrew I. Cooper, 11- 013, 128 (2007) 15721.

[8] T. Ohmori, H. Takahashi, H. Mametsuka, E. Suzuki, Physical Chemistry Chemical Physics, (2000) 3519-3522; https://doi.org/10.1039/b003977m

[9] X. Gou, G. Wang, J. Park, H. Liu, J. Yang, Nanotechnology. 19 (2008). doi:10.1088/0957-4484/19/12/125606; https://doi.org/10.1088/0957-4484/19/12/125606

[10] H. Zhou, S.S. Wong, A Facile and Mild Synthesis of 1-D ZnO , 2 (n.d.).

[11] M. Busch, M. Gruyters, H. Winter, Surf. Sci. 600 (2006) 4166-4169; https://doi.org/10.1016/j.susc.2006.01.140

[12] Supattarasakda K, Petcharoen K, Permpool T, Sirivat A,Lerdwijitjarud W (2013), Powder Technol 249:353-359; https://doi.org/10.1016/j.powtec.2013.08.042

[13] L.C. Hsu, Y.P. Kuo, Y.Y. Li, Applied Physics Letters 94 (2009) 133108 (1-3); https://doi.org/10.1063/1.3100300

[14] Sumna, S.; Chahal, S.; Kumar, A.; Kumar, P., Crystals 2020, 10, 273; https://doi.org/10.3390/cryst10040273

[15] Joseph, J.A.; Nair, S.B.; Mary, S.A.; John, S.S.; Shaji, S.; Philip, R.R., Phys. Status Solidi 2021, 259, 2100437; https://doi.org/10.1002/pssb.202100437

[16] Maki Samir A, Hassun Hanan K., Ibn AL-Haitham J Pure Appl Sci 2017;29(2):70-80.

[17] B. K. H. AL-Maiyal, B. H. Hussein, H. K. Hassun, Journal of Ovonic Research, 16 (5), (2020); https://doi.org/10.15251/JOR.2020.165.267

[18] Ayed, R.B.; Ajili, M.; Thamri, A.; Kamoun, N.T.; Abdelghani, A., Mater. Technol. 2018, 33, 769-783; https://doi.org/10.1080/10667857.2018.1503385

[19] Fareed, S.S.; Mythili, N.; Vijayaprasath, G.; Chandramohan, R.; Ravi, G., Mater. Today Proc. 2018, 5, 20955-20965; https://doi.org/10.1016/j.matpr.2018.06.485

[20] Sa. M. Alia, H. K. Hassuna, A. A. Saliha, R. H. Athabb, B. K. H. Al-Maiyalya,B. H. Hussein, Chalcogenide Letters Vol. 19, No. 10, October 2022, p. 663 – 671; https://doi.org/10.15251/CL.2022.1910.663

[21] Bushra Kadhim Hassoon Al-Maiyaly, J. for Pure & Appl. Sci. Vol.29 (3) 2016.

[22] Rihab Ben Ayed, Mejda Ajili, Yolanda Piñeiro, Badriyah Alhalaili, José Rivas, Ruxandra Vidu, Salah Kouass, Najoua Kamoun Turki, Nanomaterials 2022, 12, 1179; https://doi.org/10.3390/nano12071179

[23] Bushra H. Hussein, Hanan K. Hassun, NeuroQuantology, 18(5) (2020) 77-82; https://doi.org/10.14704/nq.2020.18.5.NQ20171

[24] B. H. Hussein, H. K. Hassun, B. K.H. Al-Maiyaly, S. H. Aleabi, Journal of Ovonic Research,

18(1),37-43 (2022); https://doi.org/10.15251/JOR.2022.181.37
[25] Hanan K. Hassun, Bushra H. Hussein, Ebtisam M.T. Salman, Auday H. Shaban, Energy Reports 6 (2020) 46-54; https://doi.org/10.1016/j.egyr.2019.10.017
[26] Nassr. I. Najm, Hanan K. Hassun, Bushra K. H. al-Maiyaly, Bushra H. Hussein, Auday H. Shaban, AIP Conference Proceedings 2123, 020031 (2019); https://doi.org/10.1063/1.5116958